Cloud Publications
International Journal of Advanced Remote Sensing and GIS
2016, Volume 5, Issue 6, pp. 1844-1858
ISSN 2320 - 0243, Crossref: 10.23953/cloud.ijarsg.64

Research Article

Open Access

Identification and Area Measurement of the Built-up Area with the Built-up Index (BUI)

Dimitris Kaimaris[1] and Petros Patias[2]

[1]School of Spatial Planning and Development (Eng.) Aristotle University of Thessaloniki, Greece
[2]School of Rural and Surveying Engineering, Aristotle University of Thessaloniki, Greece

Publication Date: 29 June 2016

DOI: https://doi.org/10.23953/cloud.ijarsg.64

Abstract The calculation and determination of the built-up area with the highest possible accuracy is of major importance in urban, suburban and agricultural studies. Until present, different methodologies of satellite image processing in their multispectral space (eg pixel-based classification) have been developed and used in Remote Sensing, allowing the identification and area measurement of the built-up area with very high accuracy. Accordingly, the indexes that have been developed are able to provide the identification and area measurement of the built-up area immediately and quickly, but with less space and measuring accuracy than other methodologies. In this paper the main indexes that are used in Remote Sensing are initially presented. Afterwards, a new index, BUI (Built-Up Index), is presented, whose development is based on the combination of the bands of Landsat ETM+: RED (band 3), SWIR1 (band 5) and SWIR2 (band 7). Its comparison with other indexes takes place in the urban, suburban and agricultural area of a Greek city, and its effectiveness is tested in four other cities (in Greece and Palestine). The results are encouraging, since this index allows the identification of the built-up area more accurately than the others. Finally, the accuracy of area measurement of the built-up area approaches accuracies obtained with other methodologies of Remote Sensing.
Keywords *Landsat ETM+; Built-up Area; Index*

1. Introduction

The identification (location, distribution and size) of the built-up area is of major importance in urban, suburban and agricultural studies. The calculation of its change throughout the time to the detriment of the non-built-up area constitutes a highly important indicator of urban change and environmental degradation (Xian and Crane, 2006; Kaufmann et al., 2007; Xu, 2008; Melesse et al., 2007; Weng, 2008). Remote sensing provides reliable scientific tools for the calculation of the built-up area, using intertemporal satellite images and studying the multispectral space. The main technics on the determination of the built-up area from satellite images utilize neural networks (Seto and Liu, 2003), supervised or unsupervised image classifications (Masek et al., 2000; Ward et al., 2000; Zhang et al., 2002; Xian and Crane, 2005; Yuan et al., 2005; Lu and Weng, 2005; Yang, 2011; Ukwattage and Dayawansa, 2012), object-based classifications (Guindon et al., 2004; Zhou et al., 2012), support vector machines (Huang and Lee, 2004; Melgani and Bruzzone, 2004; Pal and Mather, 2005; Griffiths

et al., 2010; Kamusoko et al., 2013) and Tasseled Cap transformation (Deng and Wu, 2012). Besides the above, the indexes that have been developed up to date for the determination of the built-up area are easy, rapid and, therefore, valuable tools. Their use is independent, they allow the calculation of the built-up area in a simple manner without requiring special previous satellite image processing and, lastly, they utilize multispectral bands in which there is both a strong reflection of the built-up area, and a satisfactory spectral distinction among the Earth's surface different land uses (Xu, 2010). Likewise, the images they create can be used by classification techniques to calculate the built-up area (Xu, 2007; Lee et al., 2010).

In this paper, a new combination of satellite images' bands of Landsat-7 ETM+, which can determine the built-up area as an index (BUI-Built-Up Index) directly and with satisfactory accuracy will be presented. Specifically, the following Bands are utilized: RED (band 3), SWIR1 (band 5) και SWIR2 (band 7). A comparison with the indexes that have been developed up to date is carried out in the urban, suburban and agricultural area of Thessaloniki (Central Macedonia, Greece). Moreover, the cities of Katerini (Central Macedonia, Greece), Corinth and Patras (Peloponnese, Greece) are tested in scope of proving the effectiveness of BUI.

2. Indexes and Study Area

The main Remote Sensing indexes for rapid mapping of built-up areas are the Urban Index (UI) (Kawamura et al., 1996), the Normalized Difference Built-Up Index (NDBI) (Zha et al., 2003), the Index-based Built-Up Index (IBI) (Xu, 2008), the New Built up Index (NBI) (Jieli et al., 2010) and the Enhanced Built-Up and Bareness Index (EBBI) (As-syakur et al., 2012). Landsat ETM+ bands have been used for their calculation, using the spectral regions G, R, NIR, SWIR και TIR. Particularly in the last three (NIR, SWIR και TIR) significant contrast reflection range and absorption in built-up and bare land areas is observed (Herold, 2003; Zha et al., 2003; Herold et al., 2004; Weng, 2008; Lu and Weng, 2006; As-syakur et al., 2012).

The mathematical equations between the bands of Landsat ETM+ images used for the calculation of the above indexes are presented in Table 1. Index IBI is complex, and is derived from indexes NDBI, soil adjusted vegetation index (SAVI) (Huete, 1988) and modified normalized difference water index (MNDWI) (Xu, 2005; Xu, 2006). Moreover, the normalized difference vegetation index (NDVI) can be used in index IBI (Rouse et al., 1973) instead of SAVI, when plant cover is over 30% (Ray, 1994).

Table 1: *Index Analysis*

Remote Sensing Indices	Equations between bands (Landsat 7)
UI (Urban Index)	$\frac{\text{Band 7} - \text{Band 4}}{\text{Band 7} + \text{Band 4}}$
NDBI (Normalised Difference Built-Up Index)	$\frac{\text{Band 5} - \text{Band 4}}{\text{Band 5} + \text{Band 4}}$
IBI (Index-based Built-Up Index)	$\frac{[NDBI - (SAVI + MNDWI)/2]}{[NDBI + (SAVI + MNDWI)/2]}$ If the plant cover is < 30% ; $\frac{[NDBI - (NDVI + MNDWI)/2]}{[NDBI + (NDVI + MNDWI)/2]}$ If the plant cover is ≥ 30% = $\frac{2Band5/(Band5 + Band4) - [Band4/(Band4 + Band3) + (Band2/(Band2 + Band5)]}{2Band5/(Band5 + Band4) + [Band4/(Band4 + Band3) + Band2/(Band2 + Band5)]}$
NBI (New Built up Index)	$\frac{\text{Band 3} * \text{Band 5}}{\text{Band 4}}$

EBBI (Enhanced Built-Up and Bareness Index)	$\frac{\text{Band 5} - \text{Band 4}}{10\sqrt{\text{Band 5} + \text{Band 6}}}$
Band analysis Landsat ETM+	Band 2: Visible Green (G), Spectral Range: 0.53-0.61μm
	Band 3: Visible Red (R), Spectral Range: 0.63-0.69μm
	Band 4: Near Infrared (NIR), Spectral Range: 0.78-0.90μm
	Band 5: Short Wave Infrared 1 (SWIR1), Spectral Range 1.55-1.75μm
	Band 6: Thermal Infrared (TIR), Spectral Range 10.4-12.5μm
	Band 7: Short Wave Infrared 2 (SWIR2), Spectral Range 2.09-2.35μm

The study and application area of Table's 1 indexes is the city of Thessaloniki (Central Macedonia, Greece), and its suburban and agricultural area. Thessaloniki is the second most populated city in Greece. The urban area of Thessaloniki, according to the census of 2011, has 788,952 permanent inhabitants. The prefecture of Thessaloniki has a population of 1,110,312 inhabitants, which corresponds to 9.4% of the national population. The city's position in Greece and the section of the satellite image of Landsat ETM+ (atmospherically corrected) used with elements ID: 220-336, WES P/R: 2 184/032, Acq. Date: 28/07/2005, Producer: USGS (GLCF 2014), are presented in Figures 1 and 2. Additionally, Figure 2 shows that the plant cover is over 30%, and so NDVI index will be used for the calculation of IBI. Figure 3 portrays the polygons that enclose buildings as well as the major road network of the study area, which were detected in the satellite image.

Figure 1: *Study areas*

Figure 2: *Landsat ETM+ of the city (right) of Thessaloniki and its suburban and agricultural area, false colour image RGB=421, 28/07/2005*

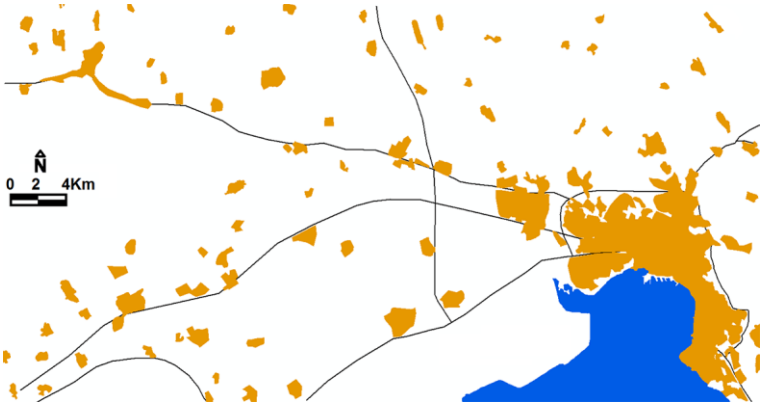

Figure 3: *Polygons enclosing buildings (continuous / discontinuous construction and the major road network of the study area*

3. Implementation of Existing Indexes and the New Index BUI

The urban, suburban and agricultural area of the study area (Figure 1 and 2) were divided into four categories/coverages, i.e., built-up area (e.g. residential, commercial, services, industrial, transportation), green vegetation (e.g. forest, shrubs and bushes, parks, cultivated land), bare soil (Ridd, 1995), and water (e.g. river, sea). In the two-dimensional spectral space, among all the combinations of Landsat ETM+ bands, the least spectral overlap between the above coverages is observed in combinations (Figure 4): RED-SWIR1, NIR- SWIR1 and SWIR1- SWIR2.

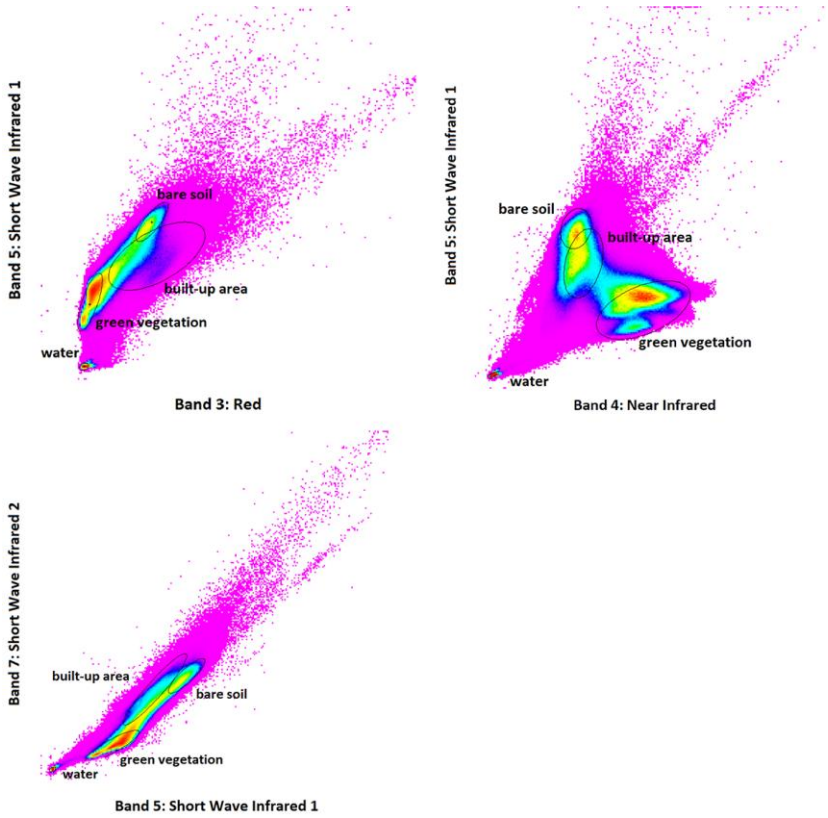

Figure 4: *Scatter plot of the four major land use classes: built-up area, green vegetation, bare soil, and water surfaces*

Optimal differentiation of the four coverages, based on the reflection of radiation (Figure 5) is observed at wavelengths NIR (Band 4) and SWIR1 (Band 5). Wavelengths RED (Band 3) and SWIR2 (Band 7) come next. In wavelength SWIR2 (Band 7) only a marginal distinction between the built-up area and the bare soil, and between green vegetation and water is observed, while the block: built-up area / bare soil is separated satisfactorily from the block: green vegetation / water. In the rest wavelengths BLUE (Band 1), GREEN (Band 2), TIR1 (Band 61) and TIR2 (Band 62), the distinction of the coverage is difficult.

The NIR spectrum region is utilized in every index of Table 2. The new index presented in this study, does not take into account this spectral region, although, as mentioned above, the region allows for the distinction of coverages (Figure 5). Specifically, among all bands of Landsat ETM+ image 4 only RED bands, SWIR1 and SWIR2 will be used, as their combination leads to a new optimal construction index. Figure 5 indicates that the subtraction of Band3 (RED) from Band5 (SWIR1) to their sum, and the addition of the subtraction of Band7 (SWIR2) from Band5 (SWIR1) to their sum, lead to high positive values for water, high negative values for bare soil and green vegetation, and minor negative values for the built-up area. Thus it becomes clear that the new index focuses on the last finding, i.e. in values ranging around 0.0, isolating the irrelevant information (green vegetation, bare soil and water) to high positive or negative values. This may not follow the logical boundary of the built-up area values adopted in indexes that have been developed so far (Ridd, 1995; Kawamura et al., 1996; Zha et al., 2003; Xu, 2007; Xu, 2008; As-syakur et al., 2012), but allows for the best distinction of constructions. The new index, BUI, is calculated according to the formula:

$$\frac{Band3 - Band5}{Band3 + Band5} + \frac{Band7 - Band5}{Band7 + Band\ 5} = \frac{2 * [(Band3 * Band7) - (Band5 * Band5)]}{(Band3 + Band5) * (Band5 + Band7)}$$

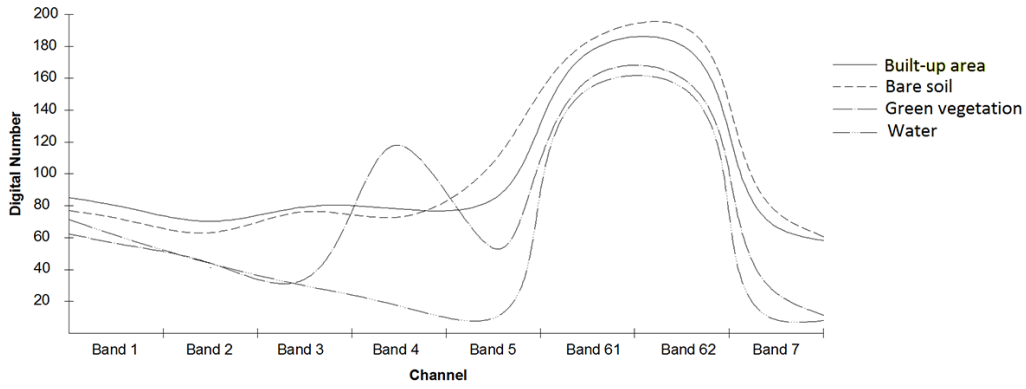

Figure 5: *Spectral profiles for four classes of land cover in Thessaloniki city and its suburban and agricultural area*

The results from the application of indexes UI, NDBI, IBI, NBI, EBBI and the new index BUI in the study area are shown in Figure 6.

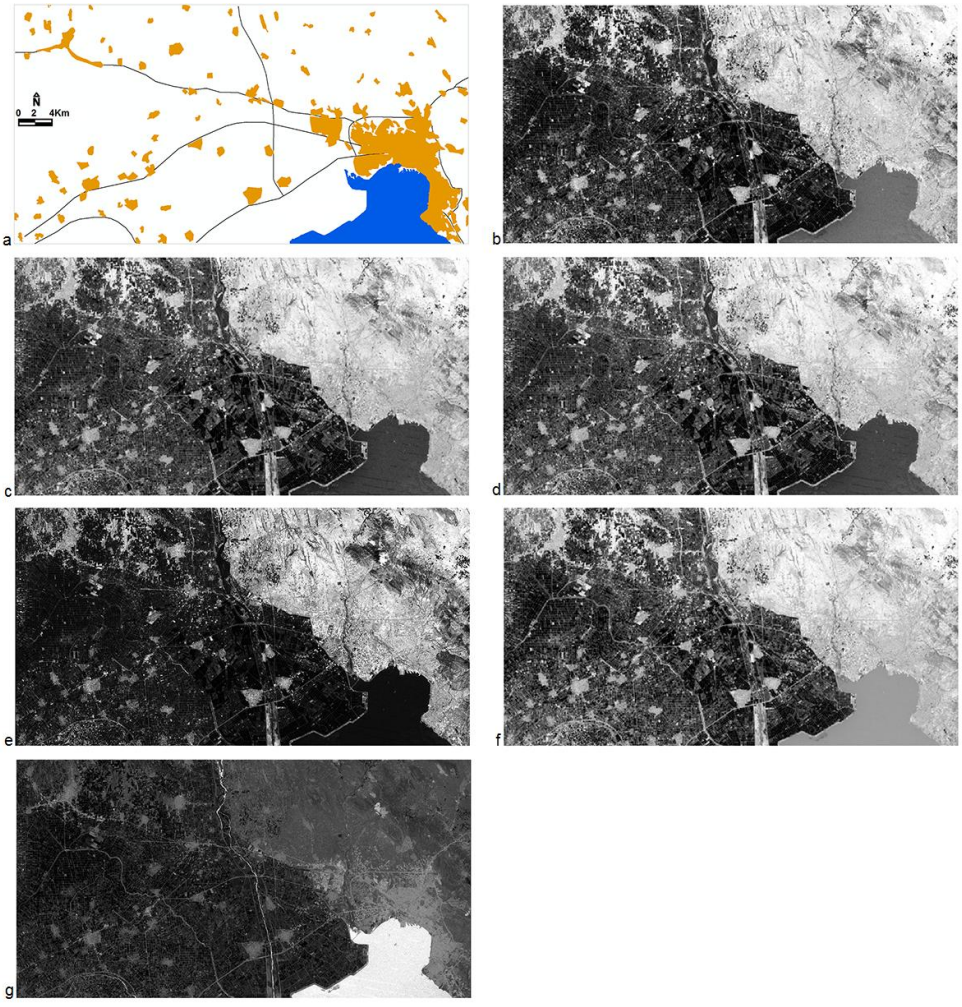

Figure 6: *The application of Table 1 indexes in the city of Thessaloniki and its suburban and agricultural area. (a) Figure 4 in reduction. (b) UI (Urban Index). (c) NDBI (Normalized Difference Built-Up Index). (d) IBI (Index-based Built-Up Index). (e) NBI (New Built up Index). (f) EBBI (Enhanced Built-Up and Bareness Index). (g) BUI (Built-Up Index)*

In scope of distinguishing the built-up area from index images (Figure 6), a minimum and maximum limit of pixel values is manually specified. In particular, the original multispectral image and the image of the index is utilized each time. Building and road positions (80-120 building and 80-120 road positions) are selected randomly but well distributed across the surface of the multispectral image. In the same positions the brightness values for each pixel of the index image are specified. These values determine the final range of the values of the index image, which corresponds to the built-up area. The range of these values for each index is presented in Table 2, and the results are the binary-images outputs shown in Figure 7.

Table 2: *Pixel values of indexes for the identification of each construction's characteristics*

Remote Sensing Indices	Between -1 - 1	Between 0 - 255
UI (Urban Index)	-0.117 - -0.008	145 - 162
NDBI (Normalised Difference Built-Up Index)	0.021 - 0.072	164 - 172
IBI (Index-based Built-Up Index)	0.027 - 0.063	184 - 190
NBI (New Built up Index)	-	70 - 100
EBBI (Enhanced Built-Up and Bareness Index)	0.127 - 0.713	122 - 130
BUI (Built-Up Index)	-0.225 - -0.013	98 - 114

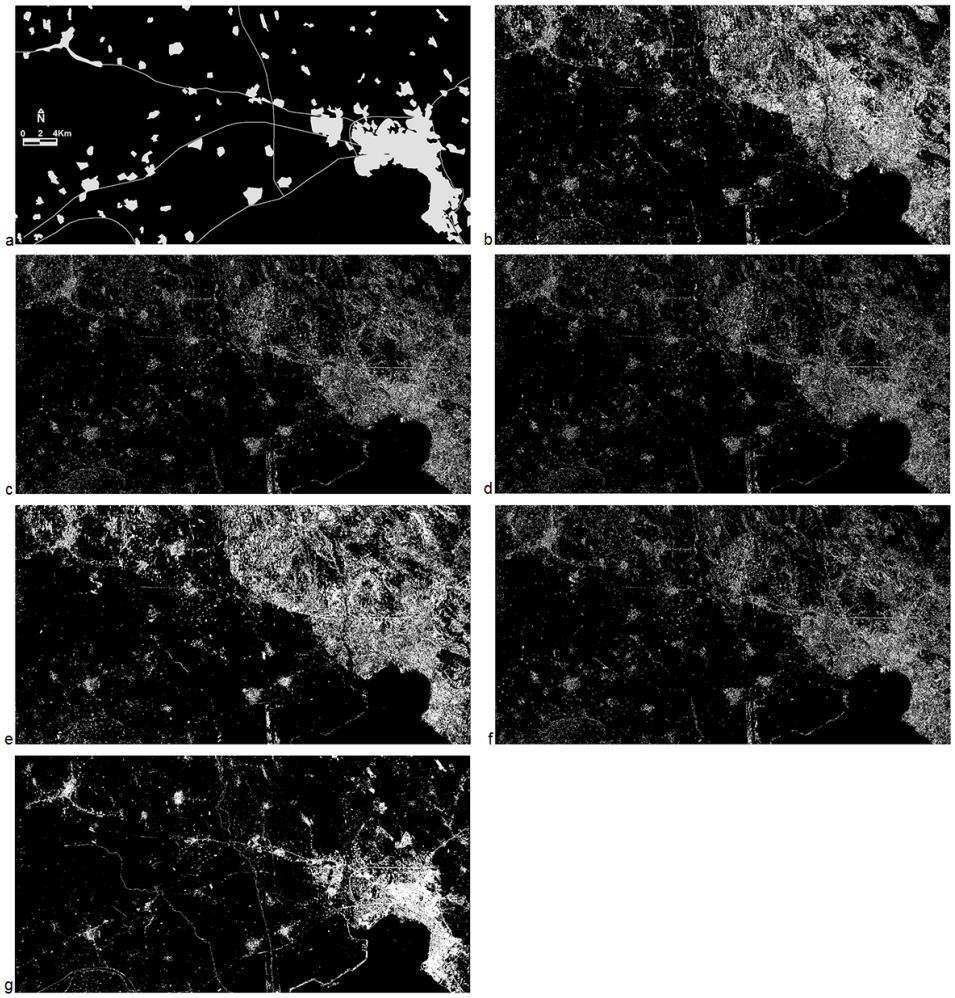

Figure 7: *Index images after the application of the brightness pixel limits for the identification of constructions. (a) Negative colours of Figure 4. (b) UI (Urban Index). (c) NDBI (Normalized Difference Built-Up Index). (d) IBI (Index-based Built-Up Index). (e) NBI (New Built up Index). (f) EBBI (Enhanced Built-Up and Bareness Index). (g) BUI (Built-Up Index)*

4. Results

For the calculation of the accuracy of the distinction between built-up area and open spaces, a random sampling method was used, and a total of 120 pixels were sampled (60 points within built-up areas, και 60 points within non built-up areas: green vegetation, bare soil, and water) in new index images (Figure 7), and compared to the corresponding points of the original Landsat ETM+ image (Figure 2). The results are presented in Table 3.

Table 3: *Index accuracy*

Remote Sensing Indices		Constructions	Not constructions	Total	User's accuracy
UI	Constructions	24	6	30	80.00%
	Not constructions	36	54	90	60.00%
	Total	60	60	120	
	Producer's accuracy	40.00%	90.00%		
	Overall accuracy	65.00%			
	Kappa	0.3000			
NDBI	Constructions	34	4	38	89.47%
	Not constructions	26	56	82	69.29%
	Total	60	60	120	
	Producer's accuracy	56.67%	93.33%		
	Overall accuracy	75.00%			
	Kappa	0.5000			
IBI	Constructions	34	2	36	94.44%
	Not constructions	26	58	84	69.05%
	Total	60	60	120	
	Producer's accuracy	56.67%	96.67%		
	Overall accuracy	76.67%			
	Kappa	0.5667			
NBI	Constructions	18	0	18	100.00%
	Not constructions	42	60	102	58.82%
	Total	60	60	120	
	Producer's accuracy	30.00%	100%		
	Overall accuracy	65.00%			
	Kappa	0.2600			
EBBI	Constructions	40	4	44	90,91%
	Not constructions	20	56	76	73,68%
	Total	60	60	120	
	Producer's accuracy	66.67%	93.33%		
	Overall accuracy	80.00%			
	Kappa	0.6000			
BUI	Constructions	50	2	52	**96.15%**
	Not constructions	10	58	68	**85.29%**
	Total	60	60	120	
	Producer's	**83.33%**	**96.67%**		

	accuracy				
	Overall accuracy	**90.00%**			
	Kappa	**0.8000**			

5. Testing the New Index in Other Areas

5.1. Built-up Area Identification

The effectiveness of the index as far as its ability to identify the built-up area is concerned (as no other measurements existed for the areas below) was tested in two other sites in Greece, in the wider region of the cities of Katerini and Corinth (Figure 1). The city of Katerini is located in Macedonia and according to 2011 census has 55,997 inhabitants. The city of Corinth is located in Peloponnese, and according to 2011 census has 30,176 inhabitants. For both regions the index led to producer's accuracies up to 82.5% and 84.2% for the built-up area (Figure 8 and 9).

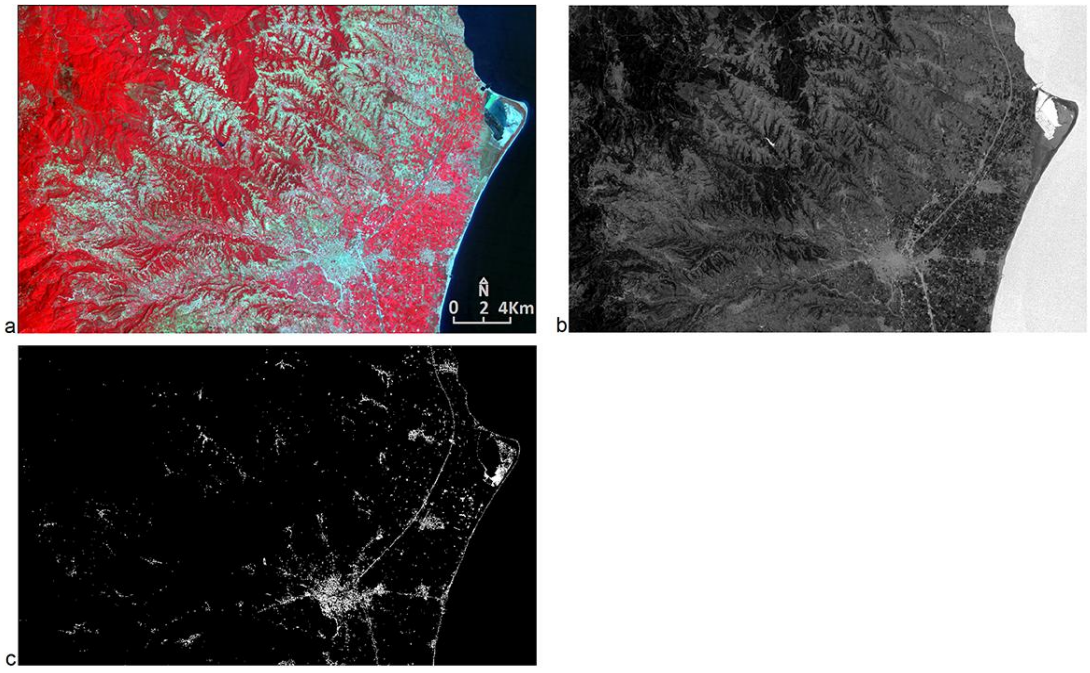

Figure 8: *(a) Landsat ETM+ (ID: 220-336, WES P/R: 2 184/032, Acq. Date: 28/07/2005, Producer: USGS), in the city of Katerini and its suburban and agricultural area. (b) The application of the new index. (c) Index image after the application of brightness pixel limits for the identification of constructions*

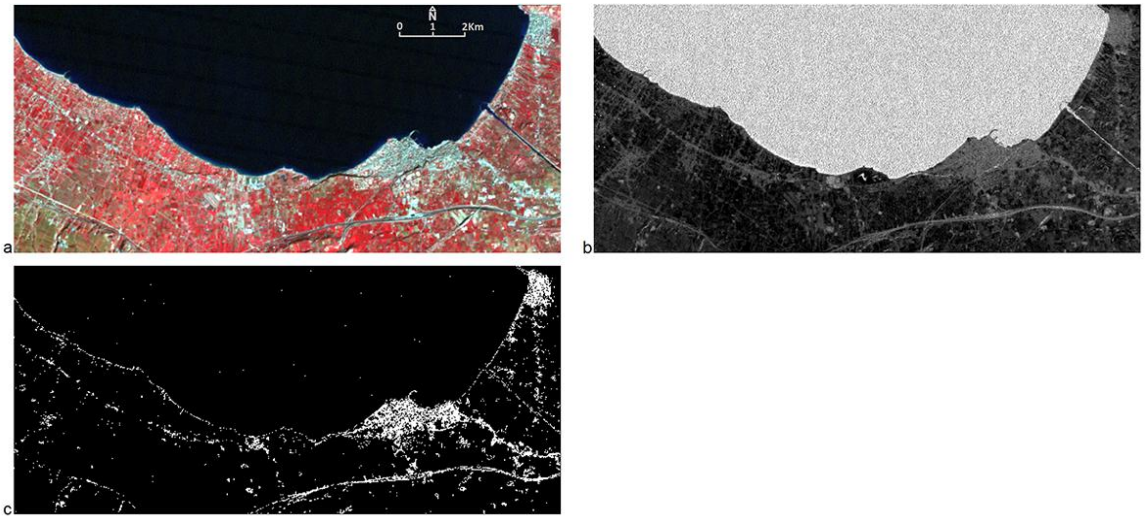

Figure 9: *(a) Landsat ETM+, (ID: 220-285, WES P/R: 2: 183/034, Acq. Date: 10/01/2005, Producer: USGS), in the city of Corinth and its suburban and agricultural area. (b) The application of the new index. (c) Index image after the application of brightness pixel limits for the identification of constructions*

5.2. Area Measurement of the Built-up Area

The index efficiency and accuracy, as far as area measurement is concerned, was tested with the use of data from the international research program LocalSats (2007-2013 ENPI CBC Mediterranean Sea Basin Programme, Table 4). The city of Patras is located in Peloponnese (Figure 1), and its urban area is the third largest area in population in Greece (according to 2011 census, the city is inhabited by 168,034 people), following the urban area of Athens and Thessaloniki. The information of Table 4 is provided by the international research program LocalSats, which is the result of modern city surveying. Bethlehem is a Palestinian city located in the central West Bank, about 10 kilometers south of Jerusalem, and has about 22,000 inhabitants. The information of Table 4 is provided by the international research program LocalSats, which is the result of photogrammetric processing of aerial images of 2010.

Table 4: *Constructions areas and boundaries within statutory urban limits*

City	Way of recording	Areas (Km^2)			
		City limits	Blocks	Buildings	Roads
Patras, Greece	Surveying (2006)	24.28	21.88	4.83	2.40
Bethlehem	Photogrammetry (2010)	5.8	3.0	2.8	

The portion of the Landsat ETM+ satellite images (atmospherically corrected) used for the city of Patras with ID elements: 220-337, WES P / R: 2: 184/033, Acq. Date: 13/08/2005, Producer: USGS (GLCF 2014), and for the city of Bethlehem (Palestine) with ID elements: 296-233, WES P / R: 2: 174/038, Acq. Date: 15/04/2010, Producer: USGS (GLCF 2014) are shown in Figures 10 (*a*) and Figure 11 (*a*) respectively. The multispectral images were corrected geometrically according to each country's national coordinate system (so that the results -areas- of the index are comparable with the data of Table 4). Afterwards, the new index BUI was applied (Figures 10 (*b*) and Figure 11 (*b*)). The minimum (Patra = 72, Bethlehem = 130) and maximum (Patra = 102, Bethlehem = 191) limits of brightness pixel values (in the range 0-255) were defined manually in scope of extracting the built-up areas from the index images (Figure 10 (*b*) and Figure 11 (*b*)). Thereafter, parts of the images enclosed within statutory limits of the urban areas were isolated (Figures 10 (*c*, *d*, *f*) and Figure 11 (*c*, *d*, *f*)). The size of the built-up area (Figure 10 (*f*)) for the city of Patras is 8.26 km^2. Compared with

Table 4 (buildings and roads cover a total area of 7.23Km^2) the area measurement error amounts to 14.2%. Finally, the size of the built-up area (Figure 11 (*e*)) for Bethlehem is 2.67 km^2, and compared to Table 4 (buildings and roads cover an area of 2.8Km^2) the area measurement error reaches 4.6%.

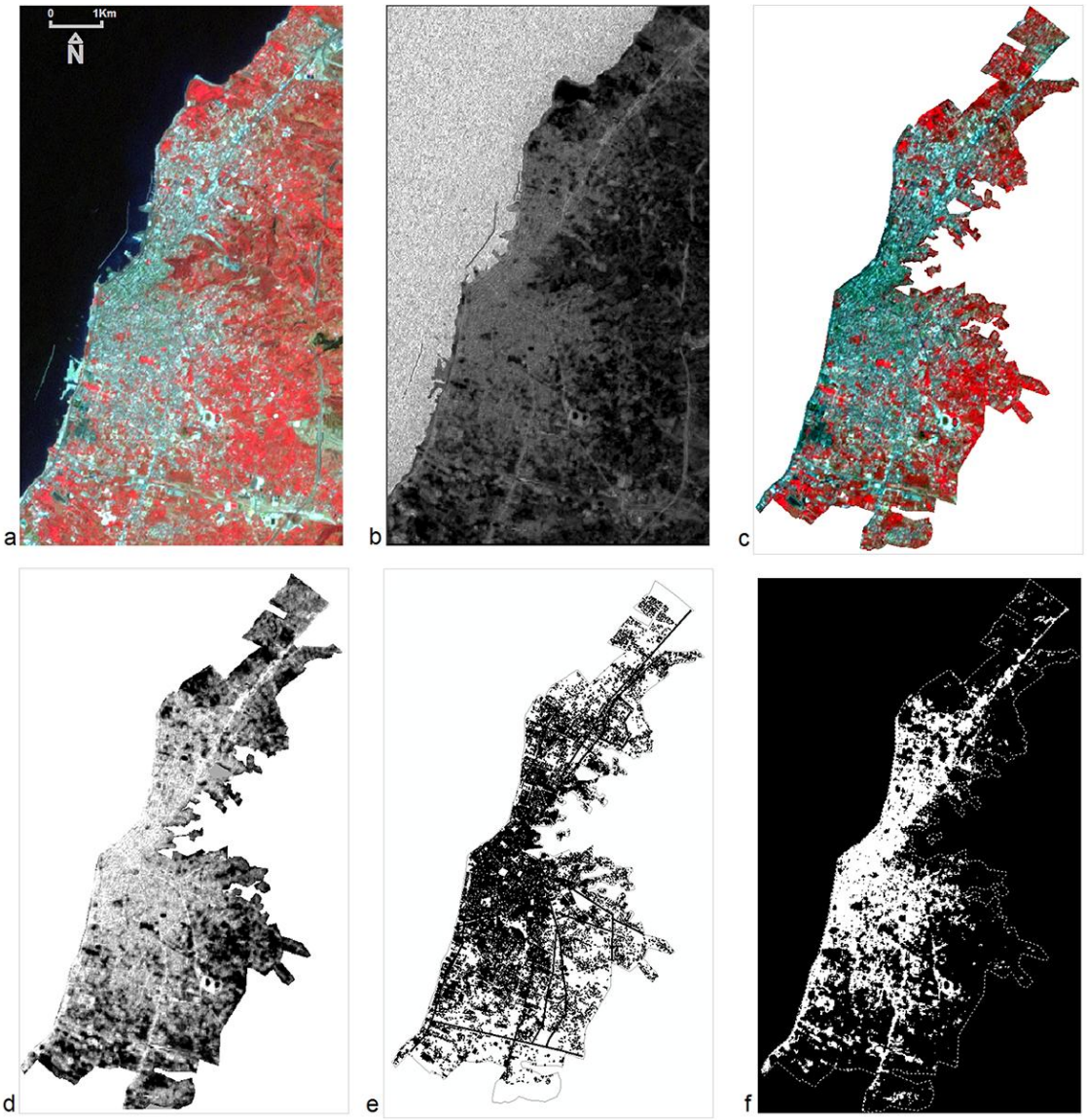

Figure 10: *(a) The multispectral satellite Landsat ETM+ image (B, G, NIR) of the city of Patras. (b) Application of BUI index. (c, d) Portion of the multispectral image (a) and the image of BUI index (b) within the statutory limits of the urban structure. (e) Surveying of buildings and roads. (f) The index image (b) after the application of brightness pixel limits to determine the built-up area within the urban area*

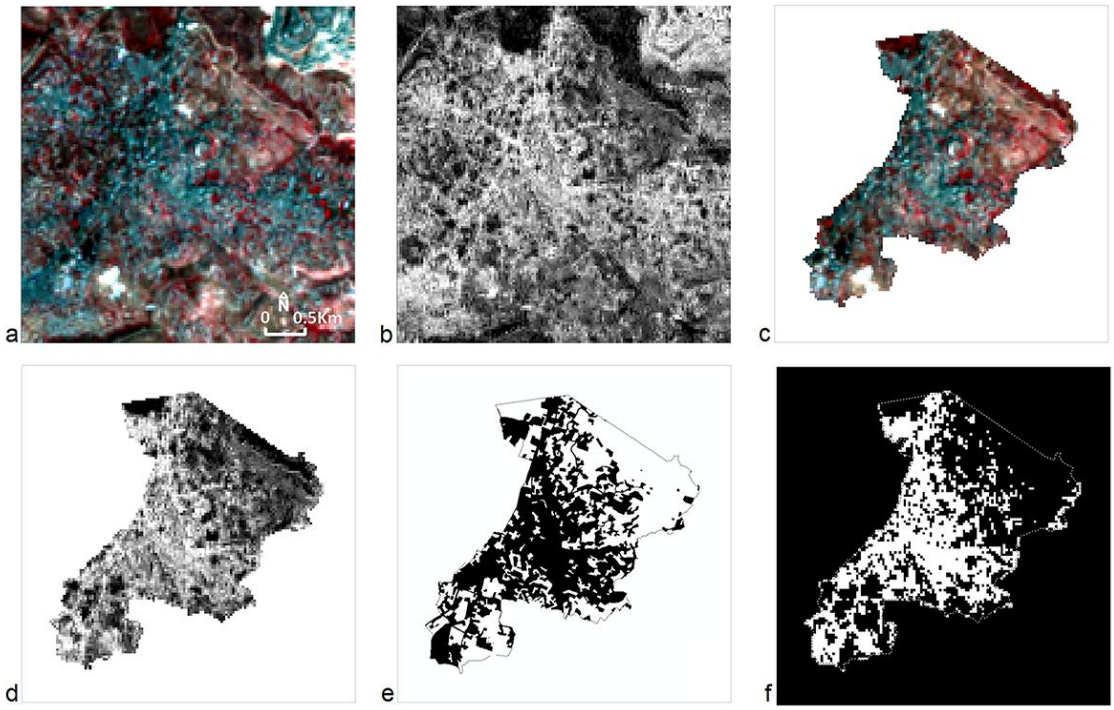

Figure 11: *(a) The multispectral satellite Landsat ETM+ image (B, G, NIR) of Bethlehem. (b) Application of BUI index. (c, d) Portion of the multispectral image (a) and the image of BUI index (b) within the statutory limits of the urban structure. (e) Surveying of buildings and roads in black. (f) The index image (b) after the application of brightness pixel limits to determine the built-up area within the urban area*

6. Conclusions

The new index BUI (Built-Up Index) which was developed and presented in this paper combines the bands of Landsat ETM+: RED (band 3), SWIR1 (band 5) and SWIR2 (band 7). NIR region of the spectrum (band 4) of the multispectral image of Landsat ETM+ was not utilized, differentiating from other indexes for the calculation of the built-up area which are developed up to date. The results of applying the index in five cities are encouraging, since the index allows the identification and area measurement of the built-up area in short time and with sufficient spatial and measuring accuracy. Specifically, the distinction accuracy (producer's accuracy) of the built-up area ranges from 82.5% to 84.2%, while the error of calculation of the area of the built-up area ranges from 4.6% to 14.2%.

Acknowledgements

We would like to thank Mona Banayout Ishaq, head of the Good Governance Program Manager, Applied Research Institute Jerusalem (ARIJ), partner of the research project LocalSats (2007-2013 ENPI CBC Mediterranean Sea Basin Programme), for the grant of geospatial data of Bethlehem (Table 4).

References

As-syakur, A.R., Adnyana, I.W.S., Arthana, I.W., and Nuarsa, I.W. *Enhanced Built-Up and Bareness Index (EBBI) for Mapping Built-Up and Bare Land in an Urban Area.* Remote Sensing. 2012. 4 (10) 2957-2970.

Deng, C. and Wu, C. BCI: *A Biophysical Composition Index for Remote Sensing of Urban Environments.* Remote Sensing of Environment. 2012. 127; 247-259.

GLCF, 2014: *Global Land Cover Facility*. Available online at: http://www.landcover.org/

Griffiths, P., Hostert, P., Gruebner, O., and Linden, S. *Mapping Megacity Growth with Multi-Sensor Data.* Remote Sensing of Environment. 2010. 114 (2) 426-439.

Guindon, B., Zhang, Y., and Dillabaugh, C. *Landsat Urban Mapping Based on a Combined Spectral-Spatial Methodology.* Remote Sensing of Environment. 2004. 92 (2) 218-232.

Herold, M., Roberts, D.A., Gardner, M.E., and Dennison, P.E. *Spectrometry for Urban Area Remote Sensing-Development and Analysis of A Spectral Library from 350 to 2400 nm.* Remote Sensing of Environment. 2004. 91; 304-319.

Herold, M., Gardner, M.E., and Roberts, D.A. *Spectral Resolution Requirements for Mapping Urban Areas.* IEEE Transactions on Geoscience and Remote Sensing. 2003. 41; 1907-1919.

Huang, Z. and Lee, G.B. *Combining Non-Parametric Models for Multisource Predictive Forest Mapping*. Photogrammetric Engineering and Remote Sensing. 2004. 70 (4) 415-425.

Huete, A.R. *A Soil-Adjusted Vegetation Index (SAVI)*. Remote Sensing of Environment. 1988. 25 (3) 295-309.

Jieli, C., Manchun, L., Yongxue, L., Chenglei, S., and Wei, H., 2010: *Extract Residential Areas Automatically by New Built up Index.* Theme Paper for the 18th International Conference on Geoinformatics, IEEE, 1-5.

Kamusoko, C., Gamba, J., and Murakami, H. *Monitoring Urban Spatial Growth in Harare Metropolitan Province, Zimbabwe.* Advances in Remote Sensing. 2013. 2; 322-331.

Kaufmann, R.K., Seto, C.K., Schneider, A., Liu, Z., Zhou, L., and Wang, W. *Climate Response to Rapid Urban Growth: Evidence of a Human-Induced Precipitation Deficit.* Journal of Climate. 2007. 20; 2299-2306.

Kawamura, M., Jayamana, S., and Tsujiko, Y. *Relation between Social and Environmental Conditions in Colombo Sri Lanka and the Urban Index Estimated by Satellite Remote Sensing Data.* Theme Paper for the International Archives of the Photogrammetry, Remote Sensing and Spatial Information Sciences. 1996. 31 (Part B7) 321-326.

Lee, A.J., Lee, S.S., and Chi, H.K. 2010: *Development of an Urban Classification Method using a Built-Up Index.* Theme Paper for the Selected Topics in Power Systems and Remote Sensing, Japan, 39-43.

Lu, D. and Weng, Q. *Urban Classification using Full Spectral Information of Landsat ETM+ Imagery in Marion County, Indiana.* Photogrammetric Engineering & Remote Sensing. 2005. 71 (11) 1275-1284.

Lu, D. and Weng, Q. *Use of Impervious Surface in Urban Land-Use Classification*. Remote Sensing of Environment. 2006. 102; 146-160.

Masek, J.G., Lindsay, F.E., and Goward, S.N. *Dynamics of Urban Growth in the Washington DC Metropolitan Area, 1973-1996, from Landsat Observations.* International Journal of Remote Sensing. 2000. 21; 3473-3486.

Melesse, A.M., Weng, Q., Thenkabail, P.S., and Senay, G.B. *Remote Sensing Sensors and Applications in Environmental Resources Mapping and Modelling*. Sensors. 2007. 7; 3209-3241.

Melgani, F. and Bruzzone, L. *Classification of Hyper-spectral Remote Sensing Images with Support Vector Machines.* IEEE Transactions on Geoscience and Remote Sensing. 2004. 42 (8) 1778-1990.

Pal, M. and Mather, M.P. *Support Vector Machines for Classification in Remote Sensing*. International of Remote Sensing. 2005. 26 (5) 1007-1011.

Ray, T.W., 1994: *A FAQ on Vegetation in Remote Sensing*. California Institute of Technology. Pasadena, California, USA.

Ridd, M.K. *Exploring a VIS (vegetation-impervious surface soil) Model for Urban Ecosystem Analysis through Remote Sensing: Comparative Anatomy for Cities.* International Journal of Remote Sensing. 1995. 16 (12) 2165-2185.

Rouse, J.W., Haas, R.H., Schell, J.A., and Deering, D.W., 1973: *Monitoring Vegetation Systems in the Great Plains with ERTS.* Theme Paper for the Third ERTS Symposium, NASA SP-351, I, 309-317.

Seto, K.C. and Liu, W. *Comparing ARTMAP Neural Network with the Maximum-Likelihood Classifier Detecting Urban Change.* Photogrammetric Engineering and Remote Sensing. 2003. 69 (9) 981-990.

Ukwattage, L.N. and Dayawansa, K.D.N. *Urban Heat Islands and the Energy Demand: An Analysis for Colombo City of Sri Lanka Using Thermal Remote Sensing Data.* International Journal of Remote Sensing and GIS. 2012. 1 (2) 124-131.

Ward, D., Phinn, R.S., and Murray, T.A. *Monitoring Growth in Rapidly Urbanizing Areas using Remotely Sensed Data*. Professional Geographers. 2000. 52 (3) 371-386.

Weng, Q., 2008: *Remote Sensing of Impervious Surfaces: An Overview*. In Remote Sensing of Impervious Surfaces; Weng, Q., (ed.) Boca Raton, FL, USA: CRC Press, Taylor & Francis Group.

Xian, G. and Crane, M. *Assessment of Urban Growth in the Tampa Bay Watershed using Remote Sensing Data.* Remote Sensing of Environment. 2005. 97 (2) 203-205.

Xian, G. and Crane, M. *An Analysis of Urban Thermal Characteristics and Associated Land Cover in Tampa Bay and Las Vegas using Satellite Data.* Remote Sensing of Environment. 2006. 104; 147-156.

Xu, H. *A Study on Information Extraction of Water Body with the Modified Normalized Difference Water Index (MNDWI).* Journal of Remote Sensing. 2005. 9 (5) 589-595.

Xu, H. *Modification of Normalized Difference Water Index (NDWI) to Enhance Open Water Features in Remotely Sensed Imagery.* International Journal of Remote Sensing. 2006. 27; 3025-3033.

Xu, H. *Extraction of Urban Built-up Land Features from Landsat Imagery using a Thematic Oriented Index Combination Technique.* Photogrammetric Engineering & Remote Sensing. 2007. 73 (12) 1381-1391.

Xu, H. *A New Index for Delineating Built-Up Land Features in Satellite Imagery*. International Journal of Remote Sensing. 2008. 29; 4269-4276.

Xu, H. *Analysis of Impervious Surface and Its Impact on Urban Heat Environment Using the Normalized Difference Impervious Surface Index (NDISI).* Photogrammetric Engineering and Remote Sensing. 2010. 76 (5) 557-565.

Yang, X. *Parameterizing Support Vector Machines for Land Cover Classification*. Photogrammetric Engineering and Remote Sensing. 2011. 77 (1) 27-37.

Yuan, F., Sawaya, E.K., Loeffelholz, C.B., and Bauer, E.M. *Land Cover Classification and Change Analysis of the Twin Cities (Minnesota) Metropolitan Area by Multitemporal Landsat Remote Sensing.* Remote Sensing of Environment. 2005. 98 (2-3) 317-328.

Zha, Y., Gao, J., and Ni, S. *Use of Normalized Difference Built-Up Index in Automatically Mapping Urban Areas from TM Imagery.* International Journal of Remote Sensing. 2003. 24; 583-594.

Zhang, Q., Wang, J., Peng, X., Gong, P., and Shi, P. *Urban Built-Up Land Change Detection with Road Density and Spectral Information from Multi-Temporal Landsat TM Data.* International Journal of Remote Sensing. 2002. 23 (15) 3057-3078.

Zhou, X., Jancsó, T., Chen, C., and Verőné, W.M., 2012: *Urban Land Cover Mapping Based on Object Oriented Classification using WorldView 2 Satellite Remote Sensing Images.* Theme Paper for the International Scientific Conference on Sustainable Development & Ecological Footprint, 1-10, Sopron, Hungary.